Int. J. Electrochem. Sci., 12 **(2017)** 8953 – 8962, doi: 10.20964/2017.10.04

International Journal of
ELECTROCHEMICAL
SCIENCE
www.electrochemsci.org

Development of a Molecularly Imprinted Electrochemical Sensor for Tert-Butylhydroquinone Recognition

Rongzhou Qin[1], *Qilin Wang*[1], *Chaoqin Ren*[1], *Xianzhi Dai*[1] *and Haijun Han*[2,*]

[1] Aba Normal University, Shuimo, Wenchuan, Aba Autonomous Prefecture of Tibetan and Qiang, Sichuan, 623001, China
[2] Sichuan University, No.24 South of the Yihuan Rd, Chengdu, Sichuan, 610065, China
[*]E-mail: hhj-zhongzhouzidao@zidao.co

Received: 30 May 2017 / *Accepted:* 24 July 2017 / *Published:* 12 September 2017

In this work, a new molecularly imprinted voltammetric sensor was fabricated based on a glassy carbon electrode (GCE) modified with reduced graphene oxide (rGO)-based silver nanoparticles (AgNPs) for the detection of tert-butylhydroquinone (TBHQ). X-ray diffraction (XRD) and X-ray photoelectron spectroscopy (XPS) techniques were used for the characterization of the proposed surfaces. The linearity range of the proposed method was determined to be 0.05-1.5 nM, and the limit of detection (LOD) was 1.48×10^{-11} M. The new voltammetric sensor exhibited remarkable recovery and selectivity for the detection of real specimens. The stability of the sensor was also investigated.

Keywords: Butylhydroquinone; Molecular imprinting; Graphene; Voltammetric sensor; Food samples

1. INTRODUCTION

It has been widely acknowledged that food quality has direct effects on human health. Food additives and antioxidants are ordinarily employed to prevent lipid-containing foods from incurring detrimental changes to their oxidisable nutrients, thus eliminating food spoilage problems. Antioxidants could be used to retard deterioration, discolouration and/or rancidity, which decreases the decay rate of oil and prolongs the shelf-life of foodstuffs and the induction period for the oxidation of lipid-containing food. Compared with natural antioxidants, synthetic phenolic antioxidants (SPA), including tert-butylhydroquinone (TBHQ), butylated hydroxyanisole (BHA) and butylated hydroxytoluene (BHT), are used more extensively, due to wide availability, chemical stability and low costs [1]. Despite the extensive use of SPAs, the safety risks cannot be neglected. It has been proposed that BHT and BHA are associated with liver damage and carcinogenesis in laboratory animals. The

criteria for whether TBHQ could be considered a food antioxidant are different from country to country. For instance, TBHQ is banned in Japan and in the European Union, whereas it can be used in foods up to a maximum concentration of 200 mg/kg in several countries, including the Philippines, New Zealand, Brazil, Australia, the United States, and China [2-5]. Therefore, it is essential to accurately detect TBHQ and other SPAs in foods when considering food safety and human health. Many different analytical techniques have been previously developed, such as UV–visible photometry [6], high-performance liquid chromatography (HPLC) [7], gas chromatography (GC) [8], and capillary electrophoresis (CE) [9]. Electrochemical techniques are considered to be excellent for detection and have been widely employed in environmental, medical, and biological detection. Electrochemical techniques also have an application in the determination of SPAs, since they are sensitive, have rapid response rates and are simple to operate [10, 11]. The molecular imprinting (MI) method is characterized by specific binding with a chemical group and is considered remarkable for the design and development of artificial receptors [12, 13].

Notably, different nanoparticles and nanomaterials could be used to develop sensitive techniques [14-18]. Moreover, significant progress in the economical production of carbon-supported materials has been made [19]. However, some significant problems remain unresolved. For instance, the catalytic performance is found to be low for detection. Therefore, new nanomaterials, including POM, carbon nanotubes and graphene/graphene oxide (GO), are becoming important for enhancing the catalytic performance [20-22]. Furthermore, mono/bimetallic particles and nanoparticles have gained great interest for use in nano/sensor technology [23]. The nanosized particles are considered to be desirable catalysts due to their larger specific surface area. In addition, the electrochemical reaction rate could also be increased by the nanoparticles [24]. POMs, which are composed of nanosized d-block transitional metal oxides, exhibit significant photocatalytic effects due to their redox features. The molecular imprinting method, formed around the analyte molecule based on polymerization, has been regarded as one of the most effective techniques for the sensitive detection [25, 26]. Specific cavities associated with the target molecule are formed by this polymerization method [27]. Due to their impermeability and resistance to high temperatures, glassy carbon electrodes have recently been extensively utilized for nanosensor applications. Nanomaterial decorated glassy carbon electrodes have been used to prepare electrochemical sensors and biosensors for the detection of environmental and biological samples. The modified glassy carbon electrode may alter electrocatalysis features, or enhance the selectivity of sensors [28-32].

The current work proposes the fabrication of the first TBHQ imprinted voltammetric sensor, and investigated its application in the detection of real specimens. The nanocomposites, including rGO, POM/rGO, and AgNPs/POM/rGO, were prepared and characterized for the first time. It is worth noting that some groups have been promoted to investigate the adsorption of POMs on several metal surfaces due to their catalytic efficacy. We also investigated the adsorption of POM (α-Keggin) on the (100) and (111) silver surfaces [33]. Based on these reports, it has been concluded that Keggin anions form ordered monolayers over silver surfaces, and their adsorption is via terminal oxo groups. Additionally, considering the affinity of Ag surfaces for oxygen atoms, the interaction was presumed to be strong and covalent on Ag surfaces [34]. The aforementioned nanomaterials were then used to modify the surface of GCE under an infrared heat lamp. Ten cycles of cyclic voltammetry (CV) were

carried out on the TBHQ imprinted surfaces after the addition of 100 mM phenol to a phosphate buffer solution (PBS) (pH 6.0) that contained 25 mM TBHQ and the AgNPs/POM/rGO modified GCE. Compared with other techniques, the proposed method was improved in its simplicity, rapidness, and ultra-sensitivity. Moreover, this method is ultra-sensitive for the detection of TBHQ in food specimens.

2. EXPERIMENTS

2.1. Reagents

Resveratrol (RES), cathecol (CAT), propyl gallate (PG), butylated hydroxyanisole (BHA), 2,6-Di-tert-butyl-4-methylphenol (BHT), activated carbon, sulphuric acid (H_2SO_4), potassium permanganate ($KMnO_4$), hydrogen peroxide (H_2O_2), isopropyl alcohol (IPA), ethanol, MeCN, silver nitrate ($AgNO_3$), graphite powder, phenol, $H_3PW_{12}O_{40}$ (POM) and tert-butylhydroquinone (TBHQ) were purchased from Sigma–Aldrich. The stock solution of BHT (1.0 mM), which was synthesized using acetonitrile (MeCN), was diluted with phosphate buffer solution (PBS) (0.1 M, pH 6.0). Sodium acetate, acetic acid, phosphorus pentoxide (P_2O_5) and potassium persulfate ($K_2S_2O_8$) were purchased from Merck (Germany).

2.2. Measurements

Electrochemical impedance spectroscopic (EIS) measurements were performed on a IVIUMSTAT & IVIUMSTAT.XR: Electrochemical Interface and Impedance Analyser. Cyclic voltammetry (CV) and differential pulse voltammetry (DPV) were performed on a C3 cell stand-equipped IviumStat (U.S). XRD analysis was performed on a Rigaku Mini X-ray diffractometer. XPS measurements were performed on a PHI 5000 Versa Probe (Φ ULVAC-PHI, Inc., Japan/USA), in which monochromatized Al Kα radiation (1486.6 eV) was applied as an X-ray anode (50 W).

2.3. Preparation of rGO, POM/rGO and AgNPs/POM/rGO

GO was prepared based on the method used in our previous study [16]. A yellow-brown suspension was obtained after dispersing the aforementioned GO into water (200 mL) under moderate ultrasound. After the addition of hydrazine hydrate (4 mL, 80 wt%), the resulting mixture was heated in an oil bath kept at 100 °C using a water-cooled condenser for 24 h. Then, the rGO product was filtered under vacuum and collected. This was followed by dissolving the as-prepared rGO into 2 mg/mL ethanol and ultrasonically agitating for 60 min. An ultra-violet (UV) light lamp was applied to reduce 1 mL of the $H_3PW_{12}O_{40}$ (1 mM). The reduced POM was added into the as-prepared rGO suspension (volume ratio, 1:1) and thoroughly mixed for 120 min to obtain the POM/rGO. This was followed by adding a 1 mM $AgNO_3$ solution to a 0.4 mg/mL POM/rGO solution (volume ratio, 1:1) in a quartz bottle. A homogeneous suspension was then obtained after sonication. The resulting solution

was then left stirring under the UV light for 40 min. Eventually, the AgNPs/POM/rGO modified GCE was obtained after dropping a AgNPs/POM/rGO (20 μL) suspension onto the electrode and was left to dry under an infrared heat lamp.

2.4. Fabrication of TBHQ imprinted voltammetric sensor

First, rGO, POM/rGO and AgNPs/POM/rGO suspensions (15 μL) were separately dropped on the bare GCE, with the solvent evaporated under an infrared lamp. Then, the modified GCE was subjected to 20 cycles of CV in the presence of 100 mM phenol in pH 6.0 PBS that contained 25 mM TBHQ (scan rate: 50 mV/s; potential range: 0.6 V to + 1.5 V) to prepare the TBHQ imprinted surface on the AgNPs/POM/rGO modified GCE (MIP/AgNPs/POM/rGO modified GCE) [35]. The TBHQ non-imprinted surface (NIP) was prepared under the same experimental conditions, but without OCH as a control experiment. There are electrostatic interactions and hydrogen bonding between the monomer and the OCH molecules. We used 1.0 M NaCl solution to break these interactions. First, the TBHQ imprinted voltammetric sensor was dipped into 30 mL of desorption agent. The electrode was then rotated in a bath (100 rpm) for 10 min. After the removal of OCH, the electrode was dried with nitrogen gas.

2.5. Preparation of food samples

The antioxidation properties of TBHQ are highly effective in grease products, especially vegetable oil. For the antioxidation of crude and refined oils, the effectiveness of TBHQ is equal or greater than that of BHT, BHA or PG. TBHQ is particularly effective in cottonseed oil, soybean oil and safflower oil. Therefore, we selected six commonly used, edible oils as food specimens, including beef tallow, colza oil, blend oil, sesame oil, arachis oil, and soybean oil. A total of 2.0 g specimens was introduced into six colourimetric cylinders (10 mL). After the addition of 5 mL of ethanol to each cylinder, the specimens in the six colourimetric cylinders were thoroughly mixed using a vortex oscillator (IKA Vortex Genius 3, Germany) and then extracted for 12 h. The supernatant (1.0 mL) was collected and transferred to a 10 mL colourimetric cylinder, then it was diluted to volume with a PBS solution and mixed to obtain the specimen solution.

3. RESULTS AND DISCUSSION

The deposition of POM on rGO sheets was carried out through electron transfer and electrostatic interactions between POM and the rGO sheets, resulting in a heterogeneous catalyst [36]. XPS was used to study the synthesis of the AgNPs/POM/rGO nanohybrid. As indicated in Fig. 1, the synthesis of AgNPs/POM/rGO was confirmed by the presence of peaks for C_{1s}, Ag_{3d}, O_{1s}, and W_{4f}. The peaks observed at 285.3, 284.2 and 283.4 eV were ascribed to –CONH, C–N and C–H in the C1s

core-level spectrum, respectively [37]. The bands observed at 366.7 and 372.6 eV were due to Ag $3d^{5/2}$ and $3d^{3/2}$ on AgNPs/POM/rGO, confirming the presence of AgNPs [14].

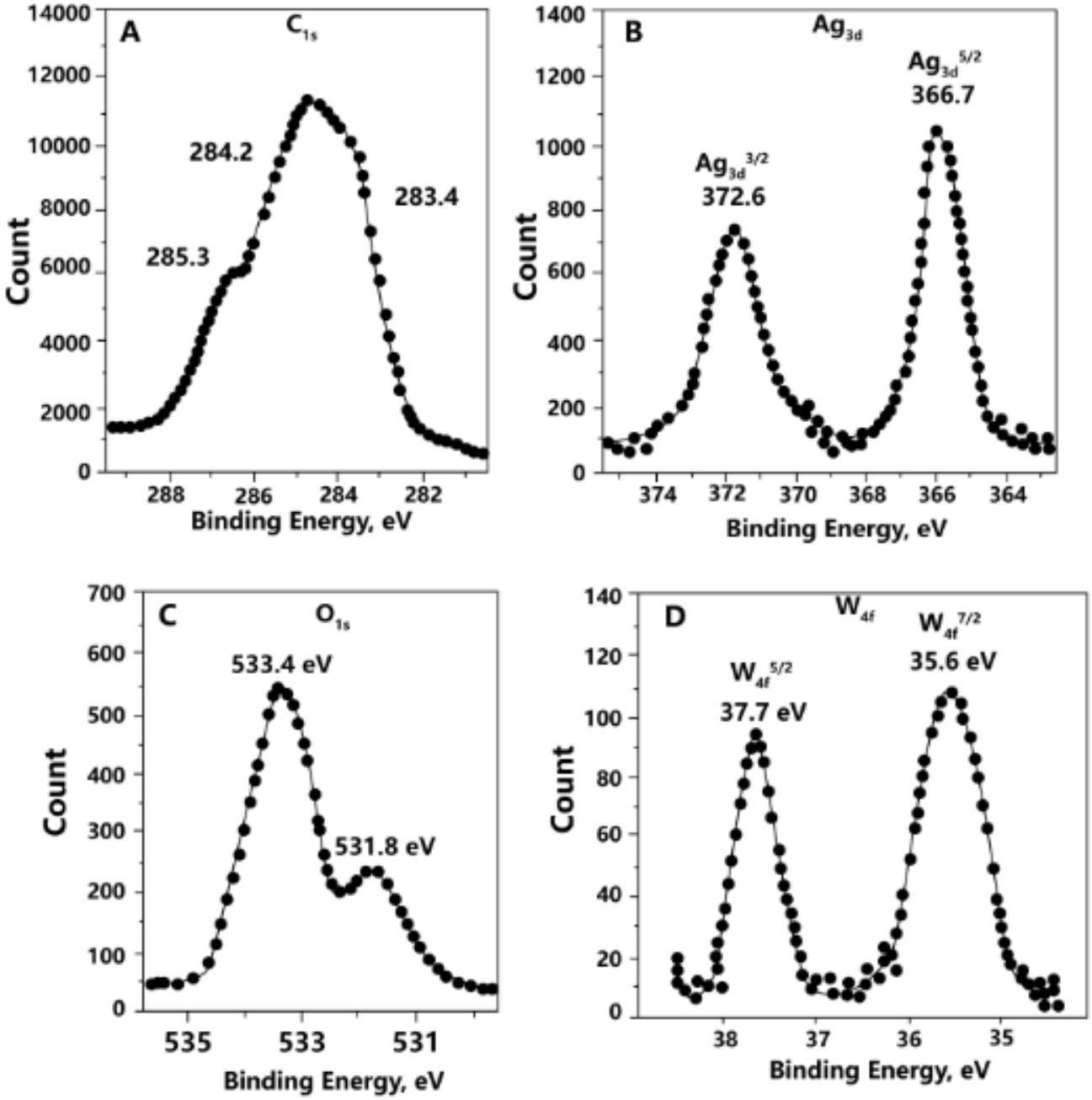

Figure 1. XPS profile of (A) C 1s, (2) Ag 3d, (C) O 1s and (D) W4f of AgNPs/POM/rGO..

Fig. 2 shows the XRD profile of AgNPs/POM/rGO. The narrow and intense peaks observed at 43.23° and 33.31° (2θ) were ascribed to the (004) and (002) planes of the rGO sheets, respectively. Furthermore, the peaks observed 42.93°, 37.05°, 27.14° and 25.02° (2θ) were ascribed to the (953), (555), (642) and (442) planes of POM, respectively. In addition, the peaks observed at 45.21° and 36.08° (2θ) referred to the (200) and (111) planes of silver, respectively.

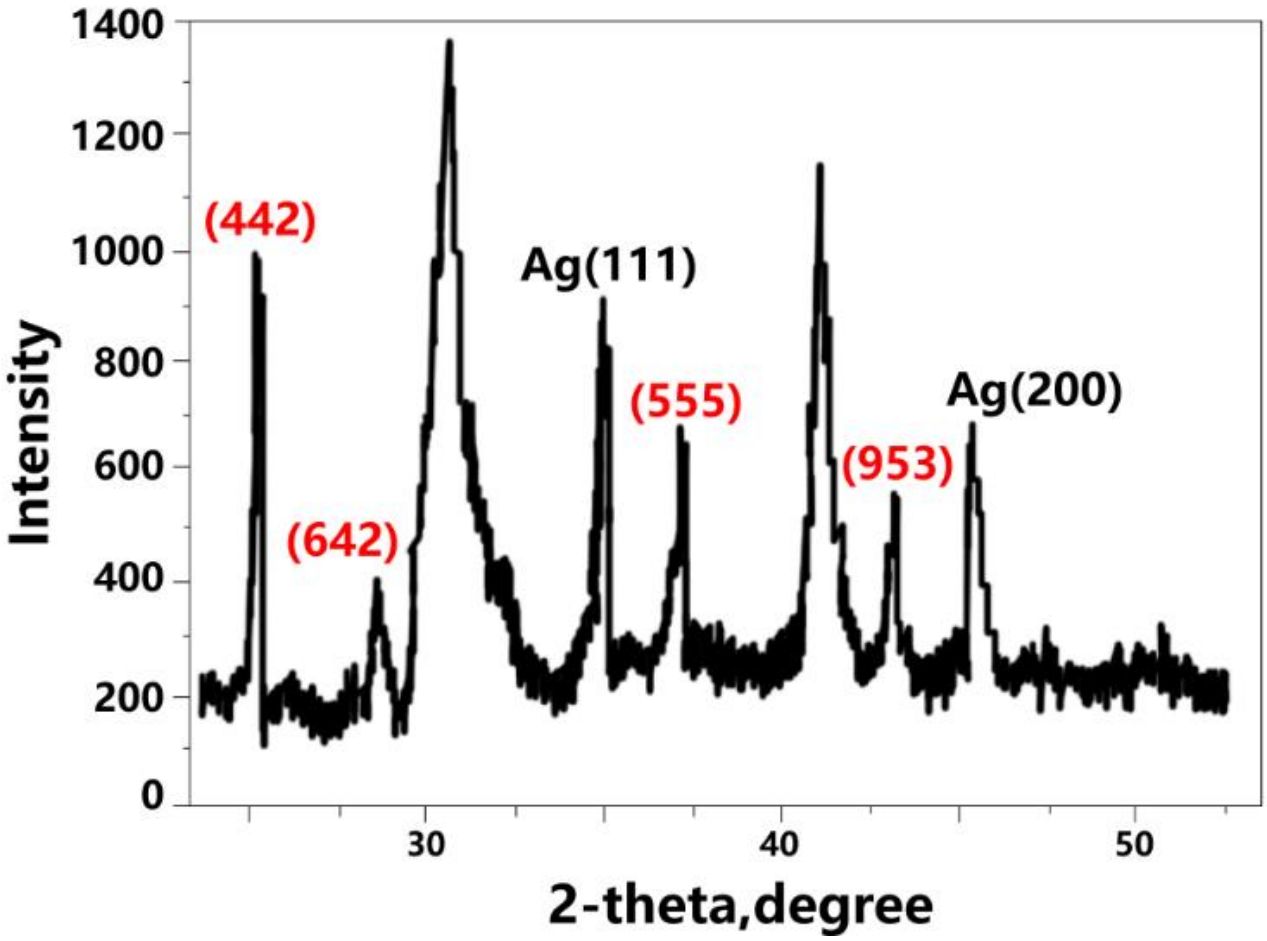

Figure 2. XRD profile of AgNPs/POM/rGO.

The original GCE exhibited a charge transfer resistance (R_{ct}) value of 110 Ω, as shown in the EIS profile in curve a (Fig. 3A). A decrease in R_{ct} (70 Ω) was observed for the rGO modified GCE, indicating that the rGO modification did not lead to the decrease in the electron transfer rate. After the rGO-modified GCE nanohybrid was modified with POM, the POM/rGO-modified GCE nanohybrid was formed. The latter nanohybrid exhibited a lower R_{ct} value compared with the former nanohybrid. A nearly-straight line was observed in the EIS profile of the AgNPs/POM/rGO-modified GCE, corresponding to a diffusion-limited step in the electrochemical process. Thus, the addition of silver nanoparticles shows an increase in the active surface area and the catalytic activity.

The MIP/AgNPs/POM/rGO-modified GCE was obtained after the polymerization of the monomer on the AgNPs/POM/rGO-modified GCE. As indicated in curve a (Fig. 3B), 675 Ω was observed for the MIP/AgNPs/POM/rGO-modified GCE, indicating the large obstruction effect by the MIP film. After the removal of TBHQ from the MIP/AgNPs/POM/rGO-modified GCE, the recognition sites for TBHQ molecules could be observed, and the R_{ct} was found to decrease to ca. 360 Ω. The R_{ct} value was then found to increase to 460 Ω after the TBHQ was reintroduced. These data indicate that the presence of TBHQ molecules hinders the electrochemical reaction of 1.0 mM $[Fe(CN)_6]^{3-/4-}$ on the electrode surface.

There were no peak currents observed for the MIP/AgNPs/POM/rGO-modified GCE in PBS (0.1 M, pH 6.0), as shown in the DPVs in Fig. 3C and 3D. After the rebinding of 1.5 nM TBHQ, a peak current was observed at ca. 1.24 V. On the other hand, a small peak current was observed for the NIP/AgNPs/POM/rGO-modified GCE, ascribed to the non-specific interaction. The current signals recorded at varying MIP electrodes were compared using DPV. Compared to the MIP-modified GCE, the MIP/rGO-modified GCE and the MIP/POM/rGO-modified GCE, the MIP/AgNPs/POM/rGO-modified GCE exhibited better performance due to its large surface area. Note that the POMs, the molecular components with high redox-activity, have the potential for the storage of electrochemical energy and the fabrication of sensors. As a class of high-valent transition metal-based anionic metal oxides, POMs may be altered in structure and reactivity over a wide range. In reduced forms, their electron and proton transfer and/or storage abilities allow them to act as efficient donors or acceptors of multiple electrons without structural change. Owing to their chemical versatility, POMs have been employed in catalysis, energy conversion and electronics [38, 39].

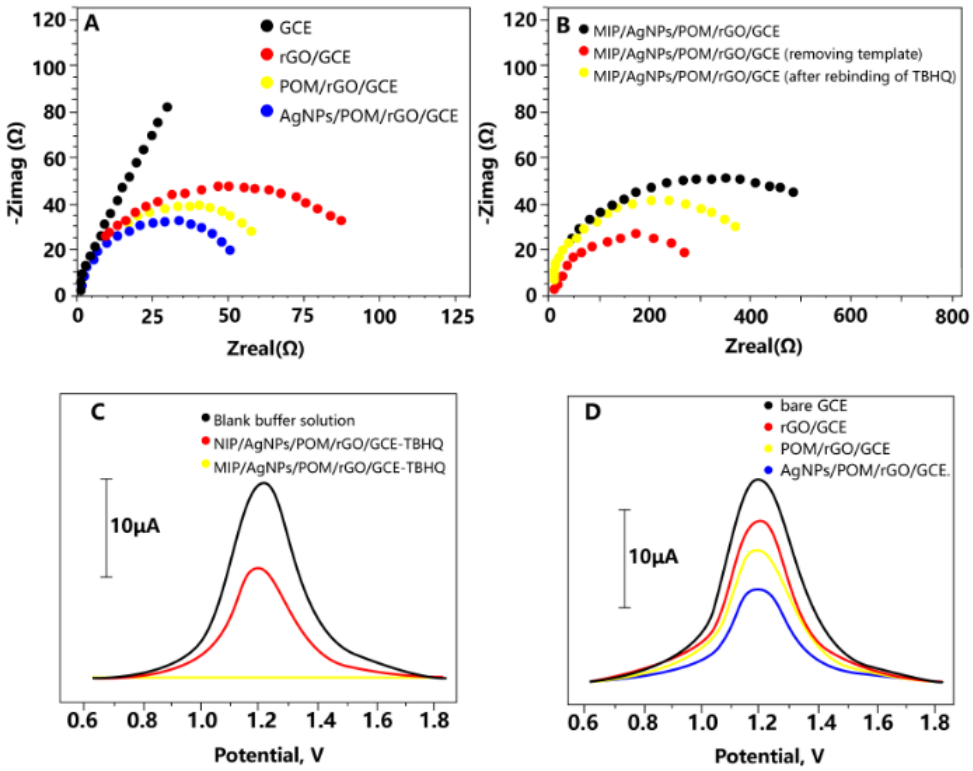

Figure 3. (A) EIS profiles of the original GCE, rGO-modified GCE, POM/rGO-modified GCE and AgNPs/POM/rGO-modified GCE in 1.0 mM $[Fe(CN)_6]^{3-/4-}$ solution in 0.1 M KCl, (B) EIS profiles of MIP/AgNPs/POM/rGO-modified GCE, MIP/AgNPs/POM/rGO-modified GCE (removing template) and MIP/AgNPs/POM/rGO-modified GCE (after the rebinding of TBHQ) in 1.0 mM $[Fe(CN)_6]^{3-/4-}$ solution in 0.1 M KCl, (C) DPV profiles of varying electrodes in PBS (0.1 M, pH 6.0): MIP/AgNPs/POM/rGO-modified GCE in a blank buffer solution, NIP/AgNPs/POM/rGO-modified GCE after the rebinding of TBHQ (1.5 nM) and MIP/AgNPs/POM/rGO-modified GCE after the rebinding of TBHQ (1.5 nM), (D) DPV profiles of varying MIP electrodes in PBS (0.1 M, pH 6.0) after the rebinding of TBHQ (1.5 nM): the original GCE, rGO-modified GCE, POM/rGO-modified GCE and AgNPs/POM/rGO-modified GCE.

As indicated by the voltammograms in Fig. 4A, an increase in the TBHQ concentration was observed, suggesting that there is a linear increase of the signal with the TBHQ concentration. The calibration profile was calculated using the mean value of six trials. As shown in Fig. 4B, the regression equation for TBHQ was expressed as follows: Y = 13.547x + 0.5022. The LOD for TBHQ was calculated to be 1.48×10^{-11} M. To allow for realistic comparison to previous reports, the characteristics of different electrochemical sensors for TBHQ are summarized in Table 1.

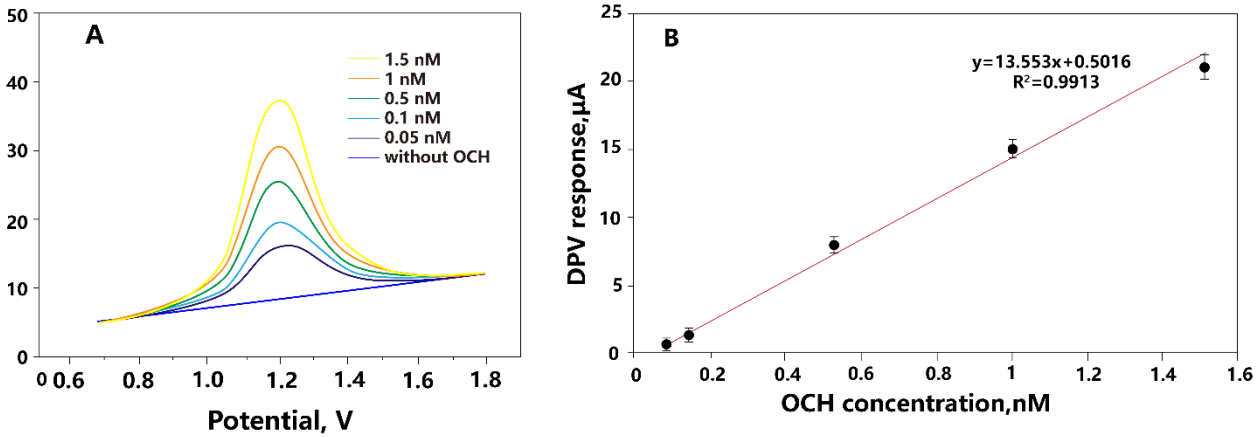

Figure 4. (A) DPV profiles for our voltammetric sensor in the presence of varying concentrations of TBHQ in PBS (pH 6.0); (B) Calibration profile for TBHQ.

Table 1. Comparison of the major characteristics of electrochemical sensors used for the detection of TBHQ.

Electrode	Linear detection range	Detection limit	Reference
Liquid chromatography/ion trap mass spectrometry	—	0.3 mg/kg	[3]
Nickel phthalocyanine complex	10-500 ppm	1.23 ppm	[40]
Normal voltammetric determination	1-15 mg/L	0.17 mg/L	[41]
AgNPs/POM/rGO modified GCE	0.05-1.5 nM	14.8 pM	This work

The response of our molecularly imprinted sensor for TBHQ (1.5 nM) was measured at three independently constructed - AgNPs/POM/rGO modified GCE to evaluate the interelectrode reproducibility of the as-prepared sensor. The relative standard deviation (RSD) was 3.7%, suggesting that the interelectrode reproducibility of our proposed sensor is favourable. A TBHQ (1.5 nM) adsorption experiment was repeated five times, and the responses were recorded to investigate the reproducibility of our proposed sensor. The RSD was ca. 4.2%, indicating that remarkable reproducibility for our proposed sensor. Moreover, the stability of the sensor was studied by detecting TBHQ after the sensor was stored at 4 °C for 30 days without use. After the first two weeks, there was no obvious decrease in the initial response. After 30 days, approximately 85% of the initial current remained. TBHQ was detected in soybean oil, blend oil and beef tallow to investigate the practical

application of our proposed electrochemical sensor in real specimen detection. The standard addition method was used for the recovery test of our sensor. The detection results are displayed in Table 2.

Table 2. Results for the detection of TBHQ in samples.

Sample	Found (nM)	RSD (%)	Added (nM)	Measured (nM)	Recovery (%)
Soybean oil	0.33	1.9	1.5	1.81	98.9
Blend oil	0.72	2.2	1.5	2.18	98.2
Beef tallow	1.43	3.6	1.5	2.97	101.4

4. CONCLUSIONS

In this work, a TBHQ imprinted voltammetric sensor was fabricated using rGO- and POM-modified AgNPs for the detection of TBHQ in grape juice and wine. The as-prepared nanomaterials were measured via several techniques. Our proposed TBHQ-imprinted voltammetric sensor was found to be sensitive for the detection of TBHQ (LOD, 1.48×10^{-11} M). Furthermore, due to high selectivity and stability, our proposed MIP sensor was shown to have a potential application in the routine detection of TBHQ in food specimens.

ACKNOWLEDGEMENT
This work was supported by grants from 2014 Key Subjects (NO.QXJ1401) of Philosophy and Social Sciences Research Base of Sichuan Province; 2014 Special Fund Project (NO.JY14-02) of Aba Normal University.

References

1. E. Almeida, F. Portela, R. Sousa, D. Daniel, M. Terrones, E. Richter and R. Muñoz, *Fuel*, 90 (2011) 3480.
2. M. Ding and J. Zou, *Food Chemistry*, 131 (2012) 1051.
3. P. Hao, J. Ni, W. Sun and W. Huang, *Food Chemistry*, 105 (2007) 1732.
4. T. Okubo, Y. Yokoyama, K. Kano and I. Kano, *Food and Chemical Toxicology*, 41 (2003) 679.
5. R. Rodil, J. Quintana, G. Basaglia, M. Pietrogrande and R. Cela, *Journal of Chromatography A*, 1217 (2010) 6428.
6. M. Komaitis and M. Kapel, *Journal of the American Oil Chemists' Society*, 62 (1985) 1371.
7. B. Saad, Y. Sing, M. Nawi, N. Hashim, A. Ali, M. Saleh, S. Sulaiman, K. Talib and K. Ahmad, *Food Chemistry*, 105 (2007) 389.
8. M. Gonzalez, M. Gallego and M. Valcarcel, *Journal of Chromatography A*, 848 (1999) 529.
9. M. Boyce and E. Spickett, *Journal of Agricultural and Food Chemistry*, 47 (1999) 1970.
10. T. De Araujo, A. Barbosa, L. Viana and V. Ferreira, *Fuel*, 90 (2011) 707.
11. R. Medeiros, R. Rocha-Filho and O. Fatibello-Filho, *Food chemistry*, 123 (2010) 886.
12. K. Haupt and K. Mosbach, *Chemical Reviews*, 100 (2000) 2495.
13. C. Xie, Z. Zhang, D. Wang, G. Guan, D. Gao and J. Liu, *Anal. Chem.*, 78 (2006) 8339.

14. M. Yola, T. Eren, N. Atar and S. Wang, *Chem. Eng. J.*, 242 (2014) 333.
15. M. Yola and N. Atar, *Electrochimica Acta*, 119 (2014) 24.
16. M. Yola, T. Eren and N. Atar, *Sensors and Actuators B: Chemical*, 210 (2015) 149.
17. H. Karimi-Maleh, F. Tahernejad-Javazmi, N. Atar, M. Yola, V. Gupta and A. Ensafi, *Ind. Eng. Chem. Res.*, 54 (2015) 3634.
18. M. Yola, T. Eren and N. Atar, *Chem. Eng. J.*, 250 (2014) 288.
19. X. Cui, L. Guo, F. Cui, Q. He and J. Shi, *J Phys Chem C*, 113 (2009) 4134.
20. M. Yola, T. Eren and N. Atar, *Electrochimica Acta*, 125 (2014) 38.
21. M. Yola, V. Gupta, T. Eren, A. Şen and N. Atar, *Electrochimica Acta*, 120 (2014) 204.
22. M. Yola, T. Eren and N. Atar, *Biosensors and Bioelectronics*, 60 (2014) 277.
23. V. Gupta, T. Eren, N. Atar, M. Yola, C. Parlak and H. Karimi-Maleh, *Journal of Molecular Liquids*, 208 (2015) 122.
24. B. Sanghavi, G. Hirsch, S. Karna and A. Srivastava, *Anal. Chim. Acta.*, 735 (2012) 37.
25. M. Yola, T. Eren and N. Atar, *Sensors and Actuators B: Chemical*, 195 (2014) 28.
26. M. Yola, V. Gupta and N. Atar, *Materials Science and Engineering: C*, 61 (2016) 368.
27. V. Gupta, M. Yola and N. Atar, *Sensors and Actuators B: Chemical*, 194 (2014) 79.
28. M. Baghayeri, E. Zare and M. Lakouraj, *Biosensors and Bioelectronics*, 55 (2014) 259.
29. M. Baghayeri, E. Zare and M. Lakouraj, *Sensors and Actuators B: Chemical*, 202 (2014) 1200.
30. M. Baghayeri, E. Zare and M. Lakouraj, *Microchim. Acta.*, 182 (2015) 771.
31. M. Musameh, J. Wang, A. Merkoci and Y. Lin, *Electrochemistry Communications*, 4 (2002) 743.
32. J. Wang, M. Li, Z. Shi, N. Li and Z. Gu, *Electroanalysis*, 14 (2002) 225.
33. C. Teague, X. Li, M.E. Biggin, L. Lee, J. Kim and A. Gewirth, *J Phys Chem B*, 108 (2004) 1974.
34. L. Lee, J. Wang, R. Adžić, I. Robinson and A. Gewirth, *Journal of the American Chemical Society*, 123 (2001) 8838.
35. V. Gupta, M. Yola, N. Özaltın, N. Atar, Z. Üstündağ and L. Uzun, *Electrochimica Acta*, 112 (2013) 37.
36. Y. Kim and S. Shanmugam, *ACS Applied Materials & Interfaces*, 5 (2013) 12197.
37. N. Atar, T. Eren, M. Yola, H. Karimi-Maleh and B. Demirdögen, *RSC Advances*, 5 (2015) 26402.
38. Y. Song and R. Tsunashima, *Chemical Society Reviews*, 41 (2012) 7384.
39. Y. Ji, T. Li and Y.-F. Song, *Ind. Eng. Chem. Res.*, 53 (2014) 11566.
40. C. Fuente, J.A. Acuña, M. Vázquez, M. Tascón and P. Sánchez Batanero, *Talanta*, 49 (1999) 441.
41. Y. Ni, L. Wang and S. Kokot, *Anal. Chim. Acta.*, 412 (2000) 185.